

Urban Heat Island Amplification Estimates on Global Warming Using an Albedo Model

Alec Feinberg

Key Words: Urban Heat Islands, Albedo Modeling, UHI Amplification Effects, UHI Heat Dome, Cool Roofs, Sea Ice Warming

Abstract In this paper, we provide nominal and worst-case estimates of radiative forcing due to UHI effect using a Weighted Amplification Albedo Solar Urbanization (WAASU) model. This calculation is done with the help of reported findings from UHI footprint and heat dome studies that simplify estimates for UHI amplification factors. Using this method, we quantify a global warming range due to the UHI effect (including urban areas). Variations in our estimates are due to urbanized area assessments and amplification factor uncertainties. However, the model showed consistent estimates of about 0.096W/m^2 per % of the normalized effective amplified area for the urbanized area feedback value. These values increase when the UHI effective contribution to climate feedback estimates are included. The model is additionally used to quantify a warming assessment due to sea ice loss. Results provide insight into the UHI area effects from a new perspective and illustrate the utility of using effective UHI amplification factors when assessing UHI's warming effect on a global scale.

1 Introduction

There are few recent publications about possible UHI influences on global warming, more up-to-date related studies, including UHI amplification effects that will be discussed in this paper, could offer supporting data for climate change theories and solutions. One key paper often referred to is by McKittrick and Michaels [1,2] who found that the net warming bias at the global level may explain as much as half the observed land-based warming. This study was criticized by Schmidt [3] and defended by Mckittrick [2] over many years. Other authors have also found significance [4-12]. These studies used land-based temperature station data to make assessments. In our study, where we introduce a Weighted Amplification Albedo Solar Urbanization (WAASU) model, we will see it has some advantages over these ground-based temperature studies. The model is non-probabilistic and in line with typical energy budget models (IPCC, Hartmann et al. [13]). It uses only two key parameters: normalized effective amplified area and average albedo. Because it is simplistic, it has transparency compared with the complex land-based studies.

The contention that UHI effects are basically only of local significance is most likely related to urban area estimates. For example, the IPCC (Satterthwaite et al. [14]) AR5 report references a Schneider et al. [15] study that resulted in urban coverage of 0.148% of the Earth (Table 1). This seemingly small area tends to dismiss the role that the UHI effect can play in large-scale global warming. Furthermore, estimates of how much land has been urbanized vary widely in the literature, in part due to the definition of what is urban and the datasets used. Although, such estimates are important for environmental studies, obtaining true estimates for the small urbanized area relative to the total land is apparently very difficult. Compounded by the fact that there is a significant difference in how groups define the term "urban". Table 1 illustrates a number of variations from select papers of interest.

In addition, global warming UHI amplification effects have not been quantified to a large degree related to area estimates. Urbanized average solar areas remain unknown.

Table 1. Urbanization area extent estimates from various sources

Percent of Land	Percent of Earth	References
2.7	0.783	GRUMP [16] – using NASA satellite light studies based on 2004 data and supplemented with census data
1	0.29	NASA [17], Galka [18] – from satellite data
0.51	0.148	Schneider et al. [15] – based on 2000-2001 data and referenced in the IPCC report (Satterthwaite, [14])
0.5	0.145	Zhou [19] – based on a 2000 data set

In our study, one key paper listed in Table 1 is due to Schneider et al. [15] since it is cited by the AR5 2014 IPCC report (Satterthwaite et al. [14]). In Schneider's paper, the larger area found in the GRUMP [16] study (Table 1) is criticized. These area estimates are of interest in our paper for the WAASU model. Additionally, the amplification factors we use are related to their urban coverage estimates.

A. Feinberg, Ph.D., DfRSoft Research, email: dfrsoft@gmail.com, ORCID: 0000-0003-4364-2460

54 In this paper we use both the Schneider et al. and GRUMP studies for the nominal and worst-cases urbanization area
 55 estimates respectively. Furthermore, they were both done using data sets near the year 2000, a good point in time to
 56 extrapolate down to 1950 and up to 2019 (see Sec. 2.5).

57
 58 **1.1 UHI Amplification Effects**
 59

60 The table below lists global warming causes and amplification effects. In this section we will summarize only the
 61 UHI amplification effects listed in the table since the root-causes and the main global warming feedback
 62 amplification effects are fairly well known.

63
 64 **Table 2.** Global warming cause and effects

Global Warming Causes →	Population → Expanding Urban Heat Islands (UHI), Roads & Increases in Greenhouse Gas
Global Warming Feedback Amplification Effects →	Water-Vapor Feedback, Land Albedo Change Due to Cities & Roads, Ice and Snow –Albedo Feedback, Lapse Rate Feedback, Cloud Feedback, etc.
Urban Heat Island Amplification Effects →	UHI Solar Heating Area (Building Areas), UHI Building Heat Capacities, Humidity Effects and Hydro-Hotspots, Reduced Wind Cooling, Solar Canyons, Loss of Wetlands, Increase in Impermeable Surfaces, Loss of Evapotranspiration Natural Cooling.

65
 66 The UHI amplification effects that we consider to dominate listed in the table are as follows:
 67

- 68 • **The humidity amplification effect:** This effect has been observed. For example, Zhao et al. [20] noted that
 69 UHI temperature increases in daytime ΔT by 3.0°C in humid climates but decreasing ΔT by 1.5°C in dry
 70 climates. They noted that such relationships imply UHIs will exacerbate heat wave stress on human health
 71 in wet UHI climates. One explanation is how heat dissipates through convection which is more difficult in
 72 humid climates. Another explanation is that warmer air holds more water-vapor. This can increase local
 73 specific humidity so that there could be local greenhouse effects.
 74
- 75 • **The heat capacity and solar heating area amplification effect:** This effect contributes to the day-night
 76 UHI cycle. In most cities, it is observed that daytime atmospheric temperatures are actually cooler
 77 compared to night. For example, in a study by Basara et al. [21] in Oklahoma city UHI, it was found that at
 78 just 9-m height, the UHI was consistently 0.5–1.75°C greater in the urban core than the surrounding rural
 79 locations at night. Further, in general UHI impact was strongest during the overnight hours and weakest
 80 during the day. This inversion effect can be the result of massive UHI buildings acting like heat sinks,
 81 having giant heat capacities and storing heat in their reservoir via convection as solar radiation is absorbed
 82 during the day. This occurrence often reduces the UHI day effect, but at night buildings cool down, giving
 83 off their stored heat that increases local temperatures to the surrounding atmosphere. This effect increases
 84 with city growth as buildings have gotten substantially taller since 1950 (Barr [22]).
 85
- 86 • **The hydro-hotspot amplification effect:** This effect is not well addressed. Atmospheric moisture source is
 87 a complex issue due to Hydro-HotSpots (HHS). HHS occurs when buildings are hot due to sun exposure.
 88 Then, during precipitation periods, the hot evaporation surfaces increase localized water-vapor as warm air
 89 holds more moisture. This increase in local greenhouse gas could blanket city heat and increase infrared
 90 radiation during these periods, providing another UHI humidity amplification source.
 91
- 92 • **Reduced wind cooling and solar canyons:** In UHIs reduced wind is a known effect due to building wind
 93 friction that inhibits cooling by convection. Tall buildings also create solar canyons and trap sunlight,
 94 reducing the average albedo, although some benefits occur from shading. In general, both have the effect of
 95 amplifying the temperature profile of UHIs.
 96

97 **2 Data and Methods**
 98

99 We see from the previous section that estimating climate change impact just based on the UHI area coverage as in
 100 Table 1, does not take into account of the effects of solar heating building sidewall areas, massive heat capacities,
 101 humidity issues, wind reduction and the solar canyon trapping that collectively amplify UHI effects beyond its own
 102 climate area.

104 2.1 UHI Area Amplification Factor

105

106 To estimate the UHI amplification effects, it is logical to first look at UHI footprint (FP) studies as they provide
 107 some measurement information. Zhang et al. [23] found the ecological FP of urban land cover extends beyond the
 108 perimeter of urban areas, and the FP of urban climates on vegetation phenology they found was 2.4 times the size of
 109 the actual urban land cover. In a more recent study by Zhou et al. [24], they looked at day-night cycles using
 110 temperature difference measurements in China. In this study, they found UHI effect decayed exponentially toward
 111 rural areas for the majority of the 32 Chinese cities. Their comprehensive study spanned from 2003 to 2012. They
 112 describe China as an ideal area to study since it has experienced the most rapid urbanization in the world in the
 113 decade they evaluated. They found that the FP of UHI effect, including urban areas, was 2.3 and 3.9 times that of
 114 urban size for the day and night, respectively. We note that the average day-night amplification footprint coverage
 115 factor is 3.1.

116 Looking at Table 2, we see that the UHI Amplification Factor (AF) is highly complex making it difficult to assess
 117 from first principles as it would be some function of Table 2 components relative to a reference year:

$$118 AF_{UHI \text{ for } 2019} = f\left(\overline{Build}_{Area} \times \overline{Build}_{C_p} \times \overline{R}_{wind} \times \overline{LossE}_{vir} \times \overline{Hy} \times \overline{S}_{canyon}\right) \quad (1)$$

119 were

120 \overline{Build}_{Area} = Average building solar area121 \overline{Build}_{C_p} = Average building heat capacity122 \overline{R}_{wind} = Average city wind resistance123 \overline{LossE}_{vir} = Average loss of evapotranspiration to natural cooling & loss of wetland124 \overline{Hy} = Average humidity effect due to hydro-hotspot125 \overline{S}_{canyon} = Average solar canyon effect

126

127 To provide some estimate of this factor, we note that Zhou et al. [24] found the FP physical area (km²), correlated
 128 tightly and positively with actual urban size having a correlation coefficients higher than 79%. This correlation can
 129 be used to provide an initial estimate of this complex factor. Therefore, as a model assumption, it seems reasonable
 130 to use area ratios for this estimate.

$$131 AF_{UHI \text{ for } 2019} = \frac{\sum (UHI \text{ Area})_{2019}}{\sum (UHI \text{ Area})_{1950}} \quad (3)$$

132 Area estimates have been obtained in the next Section in Table 3 between 2019 and 1950 time frames, yielding the
 133 following results for the Schneider et al. [15] and the GRUMP [16] extrapolated area results:

$$134 AF_{UHI \text{ for } 2019} = \frac{(Urban \text{ Size})_{2019}}{(Urban \text{ Size})_{1950}} \approx \begin{cases} \left(\frac{[0.188]_{2019}}{[0.059]_{1950}} \right)_{Schneider} = 3.19 \\ \left(\frac{[0.952]_{2019}}{[0.316]_{1950}} \right)_{GRUMP} = 3.0 \end{cases} \quad (3)$$

135 Between the two studies, the UHI area amplification factor average is 3.1. Coincidentally, this factor is the same
 136 observed in the Zhou et al. [24] study for the average footprint. This factor may seem high. However, it is likely
 137 conservative as other effects would be difficult to assess: increases in global drought due to loss of wet-lands,
 138 deforestation effects due to urbanization, and drought related fires. It could also be important to factor in changes of
 139 other impermeable surfaces since 1950, such as highways, parking lots, event centers, and so forth.

140

141 The area amplification value of 3.1 is then considered as one of our model assumptions.

142

143

144

145

146

147 **2.2 Alternate Method Using the UHI's Dome Extent**

148

149 An alternate approach to check the estimate of Equation 3, is to look at the UHI's dome extent. Fan et al. [25] using
 150 an energy balance model to obtain the maximum horizontal extent of a UHI heat dome in numerous urban areas
 151 found the nighttime extent of 1.5 to 3.5 times the diameter of the city's urban area (2.5 average) and the daytime
 152 value of 2.0 to 3.3 (2.65 average).

153

154 Applying this energy method (instead of the area ratio factor in Eq. 3, yields a diameter in 2019 compared to that of
 155 1950 with an increase of 1.8. This method implies a factor of $2.5 \times 1.8 = 4.5$ higher in the night and $2.65 \times 1.8 = 4.8$ in
 156 the day in 1950 with an average 4.65. This increase occurs 62.5% of the time according to Fan et al., where their
 157 steady state occurred about 4 hours after sunrise and 5 hours after sunset yielding an effective UHI amplification
 158 factor of 2.9. We note this amplification factor is in good agreement with Equation 3. Fan et al. [25] assessed the
 159 heat flux over the urban area extent to its neighboring rural area where the air is transported from the urban heat
 160 dome flow. Therefore the heat dome extends in a similar manner as observed in the footprint studies. If we use the
 161 dome concept, we can make an assumption that the actual surface area for the heat flux is increased by the surface
 162 area of the dome. We actually do not know the true diameter of the dome, but it is larger than the assessment by Fan
 163 et al.. Using the dome extend due to Fan et al. [25] applied to the area of diameter D , the amplification factor should
 164 be correlated to the ratios of the dome surface areas:

165

$$166 \quad AF_{UHI \text{ for } 2019} = \left(\frac{D_{2019}}{D_{1950}} \right)^2 = 2.9^2 = 8.4 \quad (4)$$

167 Thus, this equation is our second model assumption, where it is reasonable to use the ratios of the dome's surface
 168 area for an alternate approach in estimating the effective UHI amplification factor. We will have two values, 3.1 and
 169 8.4 to work with that will help in assessing model consistency and provide upper and lower bounds for effective
 170 amplification area.

171

172 **2.3 Applying the Amplification Factors**

173

174 In this analysis, 1950 is the reference year. Therefore it is not subjected to amplification. Only the new area is
 175 amplified as we are looking at changes since this time frame. This is denoted as the Amplified Affected Area
 176 (AAA). The AAA in 2019 is then given by

177

$$178 \quad AAA_{UHI \text{ for } 2019} = AF(\text{newarea}) + Area_{1950} = AF(Area_{2019} - Area_{1950}) + Area_{1950} \quad (5)$$

179 Using this, if there were no changes in UHI growth, for example so that the $Area_{2019} = Area_{1950}$, the resulting area is
 180 just the original $Area_{1950}$. This result is applied to the new area in Table 3 below.

181

182 **2.4 Area Extrapolations for 1950 and 2019**

183

184 To assess the urbanized area, (also used in determining the UHI amplification factor ratios above), we need to
 185 project the Schneider [15] and GRUMP [16] area estimates down to 1950 and up to 2019. Both use datasets are near
 186 to 2000, so this is a convenient somewhat middle time-frame. Here we decided to use the world population growth
 187 rate (World Bank [26]) which varies by year as shown in Appendix A in Figure A1. We used the average growth
 188 rate per $\frac{1}{2}$ decade for iterative projections of about 1.3% to 1.6% per year.

189

190 To justify this projection, we see that Figure A2a illustrates that building material aggregates (USGS [27]) used to
 191 build cities and roads correlates well to population growth (USGS Population Growth [28]).

192

193 It is also interesting to note that building materials for cities and roads also correlates well to global warming trends
 194 (NASA [29]) shown in Figure A2b.

195

196 Column 2 in Table 3 shows the projections with the actual year (~ 2000) data point tabulated value also listed in the
 197 table (see also Table 1). The UHI area amplification factors (Column 3) is then applied to Schneider [15] and
 198 GRUMP [16] studies shown in Column 4 using Equation 5.

199

200

201

202

203

Table 3. Extrapolated and amplified urbanized coverage estimates

Year	Urban coverage percent of Earth	Amplification factor effect	Amplification Affected Area (AAA)
Schneider study [15]			
1950	0.059*	1	0.059%
2000-2001	0.0051x29%=0.148		
2019	0.188*	3.1 AF _{Area} **	0.459%
2019	0.188*	8.4 AF _{Dome} **	1.143%
Worst-case GRUMP study [16]			
1950	0.316%*	1	0.316%
2000	0.027x29%=0.783%		
2019	0.952%*	3.1 AF _{UHI} **	2.288%
2019	0.952%*	8.4 AF _{Dome} **	5.658%

*Growth rate of cities using world population yearly growth rate in Fig A1, **AF_{UHI} is the area amplification factor for 2019 referenced to 1950.

204

205

206

207

208

2.5 Weighted Amplification Albedo Solar Urbanization (WAASU) Model Overview

209

The WAASU model is very straightforward; it is based on a global weighted albedo model. The Earth Albedo is given by

210

211

$$Earth\ Albedo = \sum_i \{ \%Effective\ Surface\ Area_i \times Surface\ Item\ Albedo_i \} + Cloud\ Area \times Cloud\ Albedo. \quad (6)$$

212

Here the effective surface area is given by

213

214

$$Effective\ Surface\ Area = Surface\ Area \times \%Solar\ Irradiance. \quad (7)$$

215

216

where the surface area includes all areas including AAA. We note that the change in the Earth Albedo over time (from 1950 to 2019), is just a function of the UHI area variation, (when holding all unrelated UHI components constant), that is

217

218

219

$$\left(\frac{dEA}{dt} \right)_{EA'} = \sum \left(Albedo_{UHI} \times \%Solar\ Irradiance \times \frac{dSurfaceArea_{UHI}}{dt} \right)_i, \quad (8)$$

220

221

where EA is the Earth's albedo (Eq. 6 and 7), and EA' is all other Earth components (held constant). Although it is possible that the solar irradiance percent changes due to new city locations, in this model we assume it is fixed at 100%. This indicates, for example, that even if we were to change the *effective Surface Area* of perhaps the *sea ice component* because it receives about 40% irradiance compared with other areas and redistributed its radiance (per the Earth's energy budget), it would not affect the overall results when looking at the albedo change over time due to the UHI effect from 1950 to 2019. Therefore, the model only requires we work with normalized area coverage changes when focusing solely on the UHI effect. On the other hand, solar irradiance comes into play for sea ice when we are considering its global albedo effect from 1950 to 2019 (see Appendix C). However, the solar radiation weighting, albedo, and areas for all Earth components are subjected to the constraints below.

222

223

224

225

226

227

228

229

230

231

2.5.1 Model Constraints

232

233

This model is subject to the constraint

234

235

$$Total\ Area = \sum_i \{ \%Normalized\ Effective\ Amplified\ Surface\ Areas_i \} + \%Cloud\ Area = 100\% \quad (9)$$

236

237

and the normalization effective amplified area (NEAA) constraint for the Earth surface areas (when the UHI area is increased) must then be subject to

238

239

$$240 \quad \sum_i \{ \% \text{ Normalized Effective Amplified Surface Areas}_i \} = 100\% - \% \text{ Cloud Area.} \quad (10)$$

241
242 To simplify things as much as possible, **only five Earth constituents are used:** *water, sea ice, land, UHI coverage,*
243 *and clouds* (where *land* is its area minus the UHI coverage). These components are fairly easy to estimate and
244 references for their values are provided in Appendix D. Furthermore, we use consistent values found in the IPCC
245 AR5 report (Hartmann et al. [13]) assessment of the Earth's energy budget for solar irradiance. Table 4 summarizes
246 the constraints from these IPCC values.

247
248 **Table 4.** IPCC Earth energy budget values (Hartmann et al. [13])

IPCC Item	Incident and Reflected Radiation (W/m ²)	Albedo %	Absorbed (W/m ²)
Earth	100/340	29.4118	240=340x(1-.294)
Atmosphere & Clouds	76/340	22.3529	79
Earth Surface Albedo	24/340	7.0588	161

249
250 The fixed components of our model maintain relative consistency from 1950 to 2019. The non-fixed value is the
251 urban coverage as indicated by Equation 8. The only unknown value is the *land* albedo (minus the UHI coverage)
252 and this value is adjusted to obtain the IPCC global albedo, 29.4118% and its *land* value of incident/reflected value
253 of 7.0588.

254
255 These values are used as a 1950 starting point and then the 2019 increase for UHI coverage area is inserted. This
256 increases the Earth's area to greater than 100%. Therefore, renormalization is done per the constraint of Equation
257 10. Renormalization is detailed in Appendix B.

258 259 **3 Results and Discussion**

260
261 Using the extrapolated area coverage in Table 3 with the 3.1 amplification factor applied to the urbanized growth,
262 the resulting global albedo change occurred of 29.3956% in 2019 (Table 5b) compared to the earlier 1950 albedo
263 value of 29.4118% (Table 5a) for the Schneider nominal case. As well, for the GRUMP worst-case, the albedo
264 changed from 29.4118% (Table 6a) to 29.3322% (Table 6b) due to the urbanized growth. Dome values are also
265 listed in the Table and for the Schneider case in Appendix B, Table B2.

266
267 As we mentioned earlier, the increases in the solar surface area of the Earth, which will occur with city growth of
268 tall buildings and their solar areas, however comparatively small, requires renormalization in the model of the Earth
269 surface components of the WAASU model (detailed in Appendix B). This information is displayed in Column 3 in
270 Tables 5b,6b and B2. While the model is sensitive to urban coverage changes, it works well with renormalization
271 showing a high level of consistency to urban coverage proportionality changes. This consistency is indicated in
272 Table 7 where we find the GRUMP [16] area feedback is 0.0944% (W/m²)/Norm Area (=0.271/2.87) compared with
273 the Schneider area feedback of 0.0948 (W/m²)/ %Norm Area (=0.055/0.58).

274
275 Table 7 provides a summary of albedo changes found in the WASSU model along with the expected solar long wave
276 radiation increase. From the above global WAASU model, the estimates of the Earth's radiated long wavelength
277 emissions are set equal to the short wave radiation absorption:

$$278 \quad P_{\text{Total}} = \mathbf{340} \text{ W/m}^2 (1 - \text{Albedo}). \quad (11)$$

280
281 Then the change from 1950 to 2019 represents the equivalent increase in long wave radiation is given by

$$282 \quad \Delta P_{\text{Total}} = \mathbf{340} \text{ W/m}^2 \{ (1 - \text{Albedo})_{2019} - (1 - \text{Albedo})_{1950} \}. \quad (12)$$

283
284
285
286
287
288
289
290

291 **Table 5a.** Schneider results (Albedo=29.4118, 1950) **Table 5b.** Schneider results (Albedo=29.3956%, 2019)

Surface	Albedo	% Area	Normalized	Weighted
	A	B	C=A x B x (1-0.67)	A x C
Sum of Water Type		71		
Sea Ice	0.6	15	4.95	2.970
Water	0.06	56	18.48	1.109
Sum of Land Type		29		
Land - (UHI + Coverage)	0.3118	28.941	9.55053	2.978
UHI + Coverage	0.12	0.059	0.01947	0.002
		Σ=100.000	33.000	7.05882
			Cloud Area	
Clouds	0.3336	67	67	22.35294
Σ Sum Earth %			100.000	
Σ Global Albedo				29.4118

Surface	Albedo	Normalized	Normalized	Weighted
	A	B	C=A x B x (1-0.67)	A x C
Sum of Water Type		70.717		
Sea Ice	0.6	14.94	4.9302	2.958
Water	0.06	55.777	18.406	1.1044
Sum of Land Type		29.283		
Land - (UHI + Coverage)	0.3118	28.826	9.513	2.966
UHI + Coverage	0.12	0.4571	0.1508	0.0181
		Σ=100.000	33.000	7.0283
			Cloud Area	
Clouds	0.3336	67	67	22.3530
Σ Sum Earth %			100.000	
Σ Global Albedo				29.3994

292

293 **Table 6a.** GRUMP results (Albedo=29.4118, 1950) **Table 6b.** GRUMP results (Albedo=29.3322%, 2019)

Surface	Albedo	% Surface Area	Normalized	Weighted
	A	B	C=A x B x (1-0.67)	A x C
Sum of Water Type		71		
Sea Ice	0.6	15	4.95	2.970
Water	0.06	56	18.48	1.109
Sum of Land Type		29		
Land - (UHI + Coverage)	0.3135	28.684	9.46572	2.968
UHI + Coverage	0.12	0.316	0.10428	0.013
Sum Surface %		Σ=100.000	33.000	7.0588
			Cloud Area	
Clouds	0.3336	67	67	22.3529
Σ Sum Earth %			100.000	
Σ Global Albedo				29.4118

Surface	Albedo	Normalized	Normalized	Weighted
	A	B	C=A x B x (1-0.67)	A x C
Sum of Water Type		69.627		
Sea Ice	0.6	14.71	4.8543	2.913
Water	0.06	54.917	18.12261	1.087
Sum of Land Type		30.3727		
Land - (UHI + Coverage)	0.3135	28.129	9.28257	2.910
UHI + Coverage	0.12	2.2437	0.740421	0.089
Sum Earth %		Σ=100.000	33.000	6.9100
			Cloud Area	
Clouds	0.3336	67	67	22.3530
Σ Sum Earth %			100.000	
Σ Global Albedo				29.3519

294

295 Results are compiled in Table 7. The table also includes “what if” estimates, if we could change urbanization to be
 296 more reflective with cool roofs to reverse the effect.

297

298 The overall results are summarized:

- 299 • Schneider nominal case from 1950 to 2019 is 0.042W/m² and 0.113W/m² due to urban area and dome
 300 amplification coverage respectively. These figures equate to about 1.18% and 3.2% of global warming
 301 assuming the total increase from 1950 is about 0.95°C in 2019.
- 302 • GRUMP worst-case from 1950 to 2019 is 0.204W/m² and 0.537W/m² due to urban area and dome
 303 amplification coverage respectively. This roughly equates to 5.7 and 15% of global warming assuming the
 304 total increase from 1950 is about 0.95°C in 2019.
- 305 • We note the consistency of the area feedback parameter having quite small variability and averaging about
 306 0.096 W/m²/ %Normalized Effective Amplified Area (%NEAA) and an average albedo feedback value of 3.4
 307 W/m²/Global Albedo change.
- 308 • “What if” corrective action results of cool roofs indicates that changing city albedos in both the Schneider
 309 and the GRUMP case from 0.12 to an average value of 0.205 would reverse the increase in emission back
 310 to 1950 levels.

311

312 Although global warming assessment obtained in the WAASU model, especially for the Schneider case does not
 313 appear to show much contribution to global warming, when contributions to climate feedback estimates are
 314 included, they show increased significance. Examples are provided in Appendix C that helps to demonstrate that
 315 when we include these feedback contributions to global warming, the UHI effect is responsible for as much as 7.3%
 316 in the Schneider case and up to 27% for the GRUMP case (see Table C4).

317

318

319

320

321
322

Table 7. Albedo and radiative increase model results with UHI effective area.

Year	Urban Extent Global Area %	UHI AEA % Area	UHI Normalized EAA Global Surface %Area	Albedo Cities	Global Weighted Albedo	ΔP_{Total} UHI Radiative Increase W/m^2 (%GW)*	Area Feedback
							$\frac{\Delta P_{Total} (W/m^2)}{\%NAAA}$ $\left(\frac{\Delta P_{Total} (W/m^2)}{\Delta Global Albedo} \right)$
Nominal Case Schneider Study							
1950	0.059	0.059	0.059	0.12	29.4118	0	—
2019	0.188	0.459 (Area AF)	0.457	0.12	29.3994	0.0422 (1.18%)*	0.092 (3.4)
2019	0.188	1.143 (Dome AF)	1.1307	0.12	29.3786	0.1129 (3.16%)*	0.1 (3.23)
What if	0.188	0.459, 1.58 (Area-Dome AF)	0.457, 1.13	0.202, 0.209	29.4118	-0.042 -1.129,	—
Worst-Case GRUMP Study							
1950	0.316%	0.316	0.316	0.12	29.4118	0	—
2019	0.952%	2.288 (Area AF)	2.2437	0.12	29.3519	0.204 (5.7%)*	0.091 (3.4)
2019	0.952%	5.658 (Dome AF)	5.395	0.12	29.2539	0.537 (15%)*	0.1 (3.4)
What if	0.952%	2.288 5.658	2.2437 5.395	0.2009, 0.2087	29.4118	-0.204 -0.537	—

*Percent of Warming estimate, $P=340 \times (1-\text{Albedo})$, $\%GW = \{(P/\epsilon\sigma)^{0.25}_{2019} - (P/\epsilon\sigma)^{0.25}_{1950}\} / 0.95^\circ\text{C}$, $\epsilon=1$

323
324
325
326

4 Conclusions

In this paper, we were able to provide estimates of UHI effect (with urban areas) on global warming. This calculation was done with the aid of assumptions for area UHI amplification factors. These estimates inserted into our WAASU model found that between 0.042W/m² to 0.537W/m² of radiative forcing is possible (this result indicates that about 1.2% to 15% of global warming may be due to the UHI effect including urban areas). This wide variation is due to both the amplification and urban area uncertainties. However, the model found that the effective UHI area feedback estimates were consistent and about 0.096W/m² per % of Normalized Effective Amplified Area. Examples are provided in Appendix C (see Table C4) to illustrate how the UHI assessment contributions can increase significantly when climate feedback problems are included. These estimates included global warming values due to the loss of sea ice over the last two decades in Appendix C; this also demonstrates the strength of the model. The final results were very dependent on UHI area estimates and amplification factors. Therefore, refined values of both would be important for future studies.

338
339

Below we provide suggestions and corrective actions which include:

- Albedo guidelines for both UHIs and roads similar to on-going CO₂ efforts.
- Guidelines for future albedo design considerations of cities.
- Recommend an agency like NASA to be tasked with finding applicable solutions to cool down UHIs.
- Recommendation for cars to be more reflective. Although world-wide vehicles likely do not embody much of the Earth’s area, recommending that all new manufactured cars be higher in reflectivity (e.g., silver or white) would help raise awareness of this issue similar to electric automobiles that help improve CO₂ emissions.

347
348
349

Appendix A: Growth Rates and Information on Natural Aggregates

Below is a plot of the world population growth rate that varies from about 2.1% to 1.1%. This graph is used to make growth rate estimates of urban coverage. We note that natural aggregates used to build cities and roads are reasonably correlated to population growth in Figure A2a. Also of interest (Fig. A2b) is the fact that one can see some correlation to global warming with the use of natural aggregates.

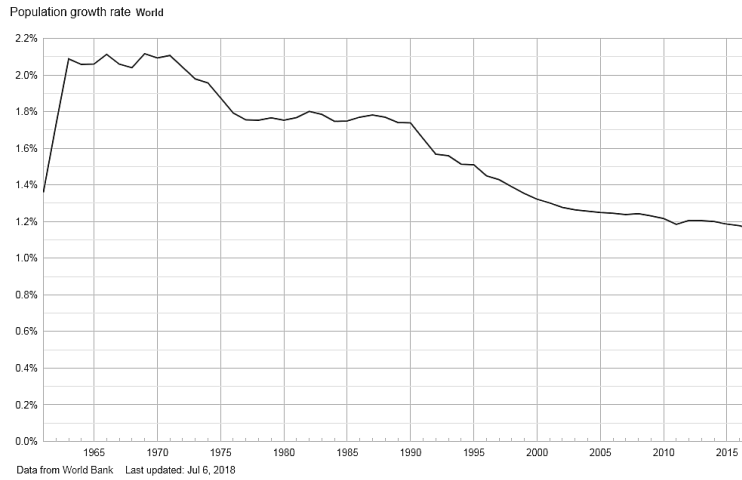


Figure A1. Population growth rate by year from 1960 to 2018, World Bank, [26]

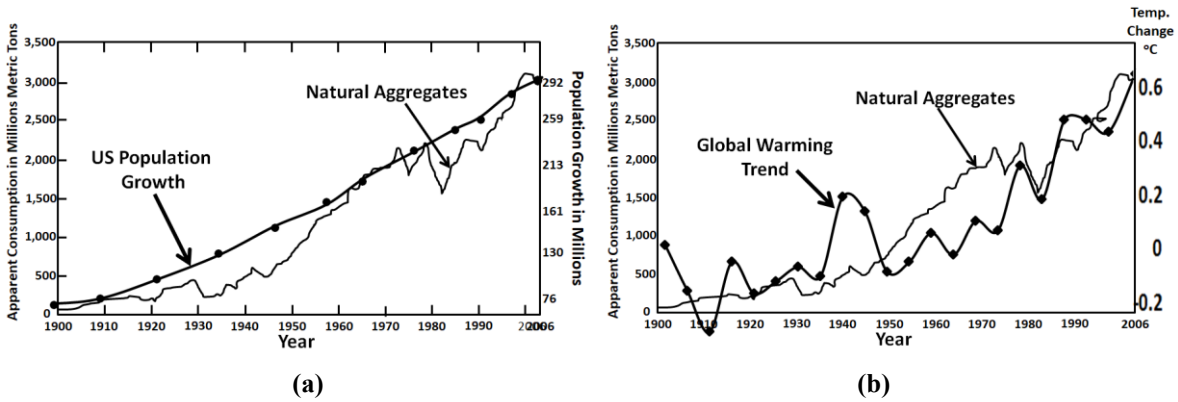


Figure A2. a) Natural aggregates [27] correlated to U.S. Population Growth (USGS [28]) b) Natural aggregates [27] correlated to global warming (NASA [29])

Appendix B: Albedo Model Normalization Information

Table 5a is reproduced from above, while Table 5b is the results of the Schneider dome area case. The results is used to demonstrate how normalization is performed

Table B1. Schneider results (Albedo=29.4118, 1950) Table B2. Schneider results (Albedo=29.3786%, 2019)

Surface	Albedo	% Area of Surface	Normalized Weighted Earth Area	Normalized Weighted Albedo %
	A	B	$C=A \times B \times (1-0.67)$	$A \times C$
Sum of Water Type		71		
Sea Ice	0.6	15	4.95	2.970
Water	0.06	56	18.48	1.109
Sum of Land Type		29		
Land - (UHI + Coverage)	0.3118	28.941	9.55053	2.978
UHI + Coverage	0.12	0.059	0.01947	0.002
		$\Sigma=100.000$	33.000	7.05882
			Cloud Area	
Clouds	0.3336	67	67	22.35294
Σ Sum Earth %			100.000	
Σ Global Albedo				29.4118

Surface	Albedo	Normalized % Surface Area	Normalized Weighted Earth Area	Normalized Weighted Albedo %
	A	B	$C=A \times B \times (1-0.67)$	$A \times C$
Sum of Water Type		70.239		
Sea Ice	0.6	14.839	4.897	2.938
Water	0.06	55.4	18.282	1.097
Sum of Land Type		29.761		
Land - (UHI + Coverage)	0.3118	28.631	9.448	2.946
UHI + Coverage	0.12	1.1307	0.373	0.0447757
		$\Sigma=100.000$	33.000	6.980769
			Cloud Area	
Clouds	0.3336	67	67	22.3530
Σ Sum Earth %			100.000	
Σ Global Albedo				29.3786

Normalization is done as follows:

1. Model starts with 1950 Table 5a albedo 29.4118%, then 2019 urban coverage area is entered.
2. For example, in Table B1, the new area increases from 0.059% to 1.143%. This value is 1.084% larger, now the 'Sum of % of Earth Area' will be 101.084% in 2019.
3. All areas are renormalized to 101.084%. For example, sea ice at 15% in 1950 becomes $15\% \times (100.000/101.084) = 14.839\%$ and the Urban Coverage becomes $1.143\% \times (100/101.084) = 1.1307\%$.

375 Appendix C: Related Warming Estimates and Other Amplification Factors

376

377 Although the results obtained here at first seem to indicate that UHIs do not appear to contribute much to global
 378 warming, when the contributions of the UHI effect to the global warming feedback problem is included, much
 379 stronger significance can be estimated. In this appendix, feedback is assessed providing a number of global warming
 380 estimates.

381

- 382 • *Such estimates are difficult to accurately calculate; however, it is not uncommon to look at how factors*
 383 *affect each other in climate science. Therefore, we have chosen to provide these in this appendix mainly*
 384 *as an aid for the reader to illustrate how climate sensitivity can factor into the magnitude of UHIs*
 385 *warming significance. These estimates should be considered only as rough approximate values.*

386

387 C.1 Global Feedback Amplification Factors

388

389 There is a wide range for possible estimates of climate feedback driven by uncertainties in how water-vapor, clouds,
 390 and other factors change as the Earth warms. Climate feedbacks are mixed and some will amplify (positive
 391 feedback) or diminish the effect of warming from the root-cause effects (for example see Hausfather [30]). The
 392 actual feedback is known to be positive (van Nes [31]). Climatologists will often approximate such factors
 393 frequently in reference to CO₂ doubling theory as positive. For example, water-vapor feedback alone, which is one
 394 of the most important in our climate system, is thought to have the capacity to approximately double the direct
 395 warming (Manabe and Wetherald [32], Randall et al [33], Dessler et. al [34]). This effect results from the fact that
 396 warm air holds more greenhouse moisture gas. Climate models incorporate this feedback. Water-vapor feedback is
 397 strongly positive, with most evidence supporting a magnitude of 1.6 to 2.0 W/m²/K (Dessler et. al. [34]). Also
 398 water-vapor feedback is considered a faster feedback mechanism (Hansen [35]). We will use a factor of 1.75, a bit
 399 less than a doubling factor of 2. This factor would apply equally to UHI warming contribution, Greenhouse Gases
 400 (GHG), or warming due to sea ice melting.

401

402 C.2 Weighted Albedo Solar Model Applied to the Melting of Sea Ice

403

404 We need to make a number of initial estimates in order to obtain a ballpark number of the warming due to sea ice
 405 loss. The first estimate is that the Antarctic sea ice has remained roughly constant (NOAA, Scott [36]) over the last
 406 two decades. Next we note that the Antarctic sea ice is larger in the winter while the Arctic sea ice is much larger in
 407 the summer. The difference appears to yield an estimate that the Arctic sea ice area is about 60% larger on average
 408 compared with Antarctic sea ice areas on a yearly basis (NOAA, Scott [36]). It has been observed that the Arctic sea
 409 ice is melting at an alarming rate of 12.85% in the last two decades (NASA sea ice [37]). This apparent trend
 410 appears to yield an estimated 26% decrease in sea ice in the last two decades. It is difficult to find a strong reference
 411 for quantifying global warming impact due to Arctic sea ice melting. However, we can get an approximation using
 412 the Weighted Albedo Solar (WAS) model (and also illustrate one of the strengths of the model). Sea ice melting will
 413 result in a significant albedo change that roughly changes the ice albedo of 0.6, to the open ocean albedo of 0.06 (see
 414 Table C1 and C2). Fortunately, the Arctic areas receive only about 40% as much solar radiation (Sciencing [38])
 415 reducing the feedback effect. From Equation 6, the effective sea ice surface area reduction from the irradiance
 416 decrease can be approximated as

417

$$418 \text{ Effective sea ice surface area} = 0.6 \times 15\% (1 - 0.26 \times 0.40) = 8.06\% \text{ (a 0.94\% reduction of effective area).} \quad (\text{C-1})$$

419

420 Here 0.6 x 15% is sea ice percent in Arctic area, 0.26 is the fraction of sea ice lost, and 40% is the solar irradiance
 421 effect. In the WAS model, we will have to make an assumption that the effective ocean surface area increases
 422 proportionately by 0.94% to 56.94% (see Table C2). The model then finds that the global albedo change decreases
 423 from 29.4118% to 29.2443%. (Note that alternately we could have set the albedo to 29.4118% in 2019 and worked
 424 back to 1950. In this case the albedo would have increased to 29.2443%).

425

426 The percent Global Warming (GW) is found as:

427

$$428 \%GW = \{(P/\epsilon\sigma)^{0.25}_{2019} - (P/\epsilon\sigma)^{0.25}_{1950}\} / 0.95^\circ\text{C}, \quad (\text{C-2})$$

429

430 where $P=340W/m^2 \times (1-Albedo)$ and $\epsilon=1$. The warming increase due to ice melting is estimated from this model to
 431 be about $0.15^\circ C$ or 15.8% of the $0.95^\circ C$ increase in 2019. The increase in radiative forcing is $0.6 W/m^2$. The
 432 feedback is then roughly $0.63 W/m^2/^\circ K$ where we assume a temperature change of $0.95^\circ C$ over this time period.
 433

434 This figure should only be taken as a rough estimate due to numerous uncertainties as climatologists find it hard to
 435 fully quantify the seasonal variations in ice change and to know the possible impact on cloud coverage increase from
 436 additional warming evaporation. However, one would expect less evaporation in the Arctic. Thus, there are a lot of
 437 uncertainties.
 438

439 **Table C1.** Schneider results (Albedo=29.4118, 1950) **Table C2.** Sea ice loss - albedo change (29.0643%, 2019)

Surface	Albedo	% Area	Normalized	Weighted
		of Surface	Earth Area	Albedo %
	A	B	$C=A \times B \times (1-0.67)$	$A \times C$
Sum of Water Type		71		
Sea Ice	0.6	15	4.95	2.970
Water	0.06	56	18.48	1.109
155Sum of Land Type		29		
Land - (UHI + Coverage)	0.3118	28.941	9.55053	2.978
UHI + Coverage	0.12	0.059	0.01947	0.002
		$\Sigma=100.000$	33.000	7.05882
			Cloud Area	
Clouds	0.3336	67	67	22.35294
Σ Sum Earth %			100.000	
Σ Global Albedo				29.4118

Surface	Albedo	Normalized	Normalized	Weighted
		% Surface Area	Earth Area	Albedo %
	A	B	$C=A \times B \times (1-0.67)$	$A \times C$
Sum of Water Type		71		
Sea Ice	0.6	14.06	4.4352	2.507
Water	0.06	56.94	18.9948	1.14
Sum of Land Type		29	23.43	
Land - (UHI + Coverage)	0.3118	28.941	9.55053	2.978
UHI + Coverage	0.12	0.059	0.01947	0.002
		100.000	33.000	6.6395
			Cloud Area	
Clouds	0.3336	67	67	22.3530
Σ Sum Earth %			123.430	
Σ Global Albedo				29.2443

440

441 **C.3 Estimated Contributions to Global Warming**

442

443 Table C3 summarizes the key global warming cause and effect factors that we have described.

444

445

Table C3. Global warming factors of interest

Urban Climate Amplification	Effects	Where Applied
UHI Area Amplification Factor	3.1 UHI Amplification	Applied to 2019 UHI Area
UHI Dome Horizontal Method	2.9 UHI Amplification	Applied to 2019 UHI Area
Ice Melting	$0.15^\circ C$	$0.15^\circ C$ out of $0.95^\circ C$
Atmospheric Moisture Increase	1.75 GW Amplification	Applied to Ice Melting Temp, UHI, and GHGs +X*

446

where X is any other feedbacks (positive or negative)

447

448 Then major contributions to global warming can be simplified as follows for the 2019 warming trend

449

$$450 \Delta T_{GW} = \Delta T_{UHI} + \Delta T_{Water-Vapor} + \Delta T_{Sea-Ice} + \Delta T_{GHG} + \Delta T_X, \tag{C-3}$$

451

452 where $\Delta T_{GW}=0.95^\circ C$, $\Delta T_{UHI-Schneider}=0.011^\circ C$ (Table 7), and $\Delta T_{Sea-Ice}=0.15^\circ C$. We have three unknowns $\Delta T_{Water-Vapor}$,

453

ΔT_{GHG} and ΔT_X . Here X is for all other feedback temperature rise due to lapse rate and increases in cloud

454

coverage and so forth. Therefore, this value can be effectively either positive or negative. The following two

455

equations will help in obtaining some estimates:

456

$$457 0.95^\circ C = AF_{water\ vapor} (\Delta T_{UHI} + \Delta T_{GHG}) + \Delta T_X + \Delta T_{Sea-Ice} = 1.75 (0.0146^\circ C + \Delta T_{GHG}) + \Delta T_X + 0.15^\circ C \tag{C-4}$$

458

and

$$459 0.95^\circ C = \Delta T_{UHI} + \Delta T_{GHG+X} + \Delta T_{Sea-Ice} + \Delta T_{Water-Vapor} = 0.0147^\circ C + \Delta T_{GHG+X} + 0.15^\circ C + \Delta T_{Water-Vapor}. \tag{C-5}$$

460

461 To obtain some example values, we need to make an assumption since we have two equations and three unknowns.

462

We will assume that T_{GHG} is 40% of global warming so that $\Delta T_{GHG}=0.38^\circ C$. Using this estimate, with the water-

463

vapor $AF_{water-vapor}=1.75$ discussed above, and equations C-4 and C5, we can obtain examples of the other

464

temperature rises due to feedbacks. These examples are provided in Table C4 for the UHI effect variations.

465
466
467
468
469
470
471
472
473
474
475

These examples illustrate the UHI effective (and urban coverage) contributions to Global Warming (GW) that occur when feedback problems are included showing this range between 2.9 to 27%.

From the table, we note UHI effective temperature rise feedback contribution factor increase of 2.43 (2.87%/1.18%), 2.3 (7.32%/3.16%), 2.2 (12.5%/5.7%), and 1.8 (27.3%/15%) with an average value of 2.2. Using this average value, it indicates that the UHI area feedback contribution could increase from 0.096W/m²/% to about 0.21W/m²/% Normalized Effective Amplified Area (see Table 7). Although these values are crude estimates, they serve as possible helpful examples.

Table C4. Global warming contributions (2019)

Warming Component	Temperature Contribution (°C)	GW Percent Root-Cause Contribution*	Percent of GW	Temperature Contribution (°C)	GW Percent Root-Cause Contribution*	Percent of GW
Schneider Study						
UHI Area Amplification=3.1				UHI Dome Amplification=8.4		
Urbanization ΔT	0.0112	2.87	1.18%	0.03	7.32	3.16%
Greenhouse gases (40%) ΔT	0.38	97.13	40.0%	0.38	92.68	40.00%
Sea ice melt feedback ΔT- rise	0.15		15.8%	0.15		15.8%
Water-vapor feedback ΔT- rise	0.3944		41.5%	0.41		43.2%
X (Other) ΔT	0.01435		1.51%	-0.02		-2.14%
Total	Σ0.95			Σ0.95		
GRUMP Study						
UHI Area Amplification=3.1				UHI Dome Amplification=8.4		
Urbanization ΔT	0.0542	12.47	5.70%	0.1425	27.27	15.00%
Greenhouse gases (35%) ΔT	0.38	87.53	40%	0.38	72.73	40.00%
Sea ice melt feedback ΔT- rise	0.15		15.8%	0.15		15.8%
Water-vapor feedback ΔT-rise	0.43		45.3%	0.51		53.2%
X (Other) ΔT	-0.065		-6.82%	-0.2275		-23.95%
Total	Σ0.95			Σ0.95		

* %ΔT_{GHG} = ΔT_{GHG} / (ΔT_{GHG} + ΔT_{Urbanization}) and %ΔT_{Urbanization} = %ΔT_{Urbanization} / (ΔT_{GHG} + ΔT_{Urbanization})

476
477
478
479
480
481
482
483
484
485

Note that the actual radiative forcing and feedback parameters are not listed but could be estimated utilizing the plank's λ_o feedback parameter and the associated temperature rises of interest in the table.

Appendix D: WAASU Model References

Table D1 provides references for the WAASU model values.

Table D1 Key References for WAASU model

Parameter	Albedo (reference)	1950 Area (reference)
Sea Ice	50-70%, average 60% (NSID [39])	15% (Lindsey [40])
Water	6% (NSID [39])	56% Ocean+Sea Ice=71% (USGS [41])
Land-(UHI+Coverage)	Adjusted to obtain 29.412% and surface reflected of 7.06 Earth Albedo in 1950 thereafter held fixed (see IPCC Hartmann [13] AR5 report)	29%-Urban Coverage
UHI+Cov	0.12 Sugawara et. Al [41]	See Table 1
Clouds	22.35294 (IPCC Hartmann et al. [13])	67% (Earthobservatory, NASA [42])
Earth Albedo	29.412% (IPCC Hartmann [13])	-

486
487
488
489
490
491

Conflicts of Interest

The author declares that he has no conflicts of interest.

References

- McKittrick R. and Michaels J. 2004. A Test of Corrections for Extraneous Signals in Gridded Surface Temperature Data, Climate Research
- McKittrick R., Michaels P. 2007 Quantifying the influence of anthropogenic surface processes and inhomogeneities on gridded global climate data, J. of Geophysical Research-Atmospheres. Also see

McKittrick Website Describing controversy: <https://www.rossmckittrick.com/temperature-data-quality.html>

- 3 Schmidt G. A. 2009 Spurious correlations between recent warming and indices of local economic activity, *Int. J. of Climatology*
- 4 Zhao, Z.-C., 1991: Temperature change in China for the last 39 years and urban effects. *Meteorological Monthly* (in Chinese), 17(4), 14-17.
- 5 Feddema, J. J., K. W. Oleson, G. B. Bonan, L. O. Mearns, L. E. Buja, G. A. Meehl, and W. M. Washington (2005), The importance of land-cover change in simulating future climates, *Science*, 310, 1674– 1678, doi:10.1126/science.1118160
- 6 Ren, G.; Chu, Z.; Chen, Z.; Ren, Y. 2007 Implications of temporal change in urban heat island intensity observed at Beijing and Wuhan stations. *Geophys. Res. Lett.* , 34, L05711,doi:10.1029/2006GL027927.
- 7 Ren, G.-Y., Z.-Y. Chu, J.-X. Zhou, et al., (2008): Urbanization effects on observed surface air temperature in North China. *J. Climate*, 21, 1333-1348
- 8 Jones, P. D., D. H. Lister, and Q.-X. Li, 2008: Urbanization effects in large-scale temperature records, with an emphasis on China. *J. Geophys. Res.*, 113, D16122, doi: 10.1029/2008JD009916.
- 9 Stone B. 2009 Land use as climate change mitigation, *Environ. Sci. Technol.*, 43(24), 9052– 9056, doi:10.1021/es902150g
- 10 Zhao, Z.-C., 2011: Impacts of urbanization on climate change. in: 10,000 Scientific Difficult Problems: Earth Science, 10,000 scientific difficult problems Earth Science Committee Eds., Science Press, 843-846. 30%
- 11 Yang, X.; Hou, Y.; Chen, B. 2011 Observed surface warming induced by urbanization in east China. *J. Geophys. Res. Atmos*, 116, doi:10.1029/2010JD015452.
- 12 Huang Q. , Lu Y. 2015 Effect of Urban Heat Island on Climate Warming in the Yangtze River Delta Urban Agglomeration in China, *Intern. J. of Environmental Research and Public Health* 12 (8): 8773 (30%)
- 13 Hartmann, D.L., A.M.G. Klein Tank, M. Rusticucci, L.V. Alexander, S. Brönnimann, Y. Charabi, F.J. Dentener, E.J. Dlugokencky, D.R. Easterling, A. Kaplan, B.J. Soden, P.W. Thorne, M. Wild and P.M. Zhai, 2013: Observations: Atmosphere and Surface. In: *Climate Change 2013: The Physical Science Basis. Contribution of Working Group I to the Fifth Assessment Report of the Intergovernmental Panel on Climate Change* [Stocker, T.F., D. Qin, G.-K. Plattner, M. Tignor, S.K. Allen, J. Boschung, A. Nauels, Y. Xia, V. Bex and P.M. Midgley (eds.)]. Cambridge University Press, Cambridge, United Kingdom and New York, NY, USA.
- 14 Satterthwaite D.E., F. Aragón-Durand, J. Corfee-Morlot, R.B.R. Kiunsi, M. Pelling, D.C. Roberts, and W. Solecki, 2014: Urban areas. In: *Climate Change 2014: Impacts, Adaptation, and Vulnerability. Part A: Global and Sectoral Aspects. Contribution of Working Group II to the Fifth Assessment Report of the Intergovernmental Panel on Climate Change (IPCC)*
- 15 Schneider,A., M. Friedl, and D. Potere, 2009:A new map of global urban extent from MODIS satellite data. *Environmental Research Letters*, 4(4), 044003, doi:10.1088/ 1748-9326/4/4/044003
- 16 Global Rural Urban Mapping Project (GRUMP) 2005, Columbia University Socioeconomic Data and Applications Center, Gridded Population of the World and the Global Rural-Urban Mapping Project (GRUMP).
- 17 NASA 2000, Gridded population of the world, , <https://sedac.ciesin.columbia.edu/data/set/gpw-v3-population-count/data-download>
- 18 Galka M. 2016, Half the World Lives on 1% of Its Land, Mapped, <https://www.citylab.com/equity/2016/01/half-earth-world-population-land-map/422748/>, , (2016 publication on 2000 data set, <http://metrocosm.com/world-population-split-in-half-map/>
- 19 Zhou Y. , Smith S. , Zhao K. , M. Imhoff, A. Thomson, B. Lamberty,G. Asrar, X. Zhang, C. He and C. Elvidge, A global map of urban extent from nightlights, *Env. Research Letters*, 10 (2015), (study uses a 2000 data set).
- 20 Zhao L, Lee X, Smith RB, Oleson K, Strong 2014, contributions of local background climate to urban heat islands, *Nature*. 10;511(7508):216-9. doi: 10.1038/nature13462
- 21 Basara J. ,P. Hall Jr. , A.Schroeder , B.Illston ,K.Nemunaitis 2008, Diurnal cycle of the Oklahoma City urban heat island, *J. of Geophysical Research*
- 22 Barr J. M., 2019 The Economics of Skyscraper Height (Part IV): Construction Costs Around the World, <https://buildingtheskyline.org/skyscraper-height-iv/>
- 23 Zhang, X., Friedl, M. A., Schaaf, C. B., Strahler, A. H. & Schneider, A. 2004 The footprint of urban climates on vegetation phenology. *Geophys. Res. Lett.* 31, L12209
- 24 Zhou D. , Zhao S. , L. Zhang, G Sun and Y. Liu, 2015, The footprint of urban heat island effect in China, *Scientific Reports*. 5: 11160
- 25 Fan, Y., Li, Y., Bejan, A. et al. Horizontal extent of the urban heat dome flow. *Sci Rep* 7, 11681 (2017). <https://doi.org/10.1038/s41598-017-09917-4>

- 26 World Bank, 2018 population growth rate, worldbank.org
- 27 USGS 1900-2006, Materials in Use in U.S. Interstate Highways, <https://pubs.usgs.gov/fs/2006/3127/2006-3127.pdf>
- 28 US Population Growth 1900-2006, u-s-history.com/pages/h980.html
- 29 NASA 1900-2006 updated, 2020 <https://climate.nasa.gov/vital-signs/global-temperature/>
- 30 Hausfather Z., (2018) *How Scientist Estimate Climate Sensitivity*, in *Carbon Brief*, <https://www.carbonbrief.org/explainer-how-scientists-estimate-climate-sensitivity>
- 31 van Nes E. H., Scheffer M., Brovkin V., Lenton T. M., Ye H, Deyle E. and Sugihara G., *Nature Climate Change* 2015. [dx.doi.org/10.1038/nclimate2568](https://doi.org/10.1038/nclimate2568)
- 32 Manabe, S., and R. T. Wetherald (1967), Thermal equilibrium of atmosphere with a given distribution of relative humidity, *J. Atmos. Sci.*, 24, 241–259.
- 33 Randall, D. A. et al. (2007), Climate models and their evaluation, in *Climate Change 2007: The Physical Science Basis. Contributions of Working Group I to the Fourth Assessment Report of the Intergovernmental Panel on Climate Change*, edited by S. Solomon et al., pp. 591–662, Cambridge Univ. Press, Cambridge, U.K.
- 34 Dessler A. E. ,Zhang Z., Yang P., Water-vapor climate feedback inferred from climate fluctuations, 2003–2008, *Geophysical Research Letters*, (2008), <https://doi.org/10.1029/2008GL035333>
- 35 Hansen, J., "2008: Tipping point: Perspective of a climatologist." Archived 2011-10-22 at the Wayback Machine, *Wildlife Conservation Society/Island Press*, 2008. Retrieved 2010.
- 36 NOAA, Scott, M, 2019, Understanding Climate:Antarctic sea ice extent, <https://www.climate.gov/print/833949>
- 37 NASA Sea Ice, 2019, <https://climate.nasa.gov/vital-signs/arctic-sea-ice/>
- 38 Sciencing (2018) <https://sciencing.com/sun-intensity-vs-angle-23529.html>
- 39 NSID 2020, National Snow & Ice Data Center, "Thermodynamics: Albedo". [nsidc.org](https://nsidc.org/cryosphere/seaice/processes/albedo.html). Retrieved 14 August 2016. <https://nsidc.org/cryosphere/seaice/processes/albedo.html>
- 40 Lindsey R, Scott M., (2019), Climate Change: Arctic Sea Ice Summer Minimum, NOAA Climate.gov, <https://www.climate.gov/news-features/understanding-climate/climate-change-minimum-arctic-sea-ice-extent>
- 41 Sugawara, H., Takamura, T. Surface Albedo in Cities (0.12): Case Study in Sapporo and Tokyo, Japan. *Boundary-Layer Meteorol* 153, 539–553 (2014). <https://doi.org/10.1007/s10546-014-9952-0>
- 41 USGS on Amount of Earth covered by water, https://www.usgs.gov/special-topic/water-science-school/science/how-much-water-there-earth?qt-science_center_objects=0#qt-science_center_objects
- 42 Earthobservatory, NASA (clouds albedo 0.67) <https://earthobservatory.nasa.gov/images/85843/cloudy-earth>

492
493
494
495
